BIOTECHNOLOGY

Field-deployable viral diagnostics using CRISPR-Cas13

Cameron Myhrvold,[1,2]*† Catherine A. Freije,[1,2,3]*† Jonathan S. Gootenberg,[1,4,5,6,7]‡ Omar O. Abudayyeh,[1,5,6,7,8]‡ Hayden C. Metsky,[1,9] Ann F. Durbin,[3,10] Max J. Kellner,[1] Amanda L. Tan,[11] Lauren M. Paul,[11] Leda A. Parham,[12] Kimberly F. Garcia,[12] Kayla G. Barnes,[1,2,13] Bridget Chak,[1,2] Adriano Mondini,[14] Mauricio L. Nogueira,[15] Sharon Isern,[11] Scott F. Michael,[11] Ivette Lorenzana,[12] Nathan L. Yozwiak,[1,2] Bronwyn L. MacInnis,[1,13] Irene Bosch,[10,16] Lee Gehrke,[3,10,17] Feng Zhang,[1,5,6,7] Pardis C. Sabeti[1,2,3,13,18]†

Mitigating global infectious disease requires diagnostic tools that are sensitive, specific, and rapidly field deployable. In this study, we demonstrate that the Cas13-based SHERLOCK (specific high-sensitivity enzymatic reporter unlocking) platform can detect Zika virus (ZIKV) and dengue virus (DENV) in patient samples at concentrations as low as 1 copy per microliter. We developed HUDSON (heating unextracted diagnostic samples to obliterate nucleases), a protocol that pairs with SHERLOCK for viral detection directly from bodily fluids, enabling instrument-free DENV detection directly from patient samples in <2 hours. We further demonstrate that SHERLOCK can distinguish the four DENV serotypes, as well as region-specific strains of ZIKV from the 2015–2016 pandemic. Finally, we report the rapid (<1 week) design and testing of instrument-free assays to detect clinically relevant viral single-nucleotide polymorphisms.

Recent viral outbreaks have highlighted the challenges of diagnosing viral infections, particularly in areas far from clinical laboratories. Viral diagnosis was especially difficult during the 2015–2016 Zika virus (ZIKV) pandemic; low viral titers and transient infection (*1*, *2*), combined with limitations of existing diagnostic technologies, contributed to ZIKV circulating for months before the first cases of infection were confirmed clinically (*3*–*5*). An additional challenge for viral diagnostics is differentiating between related viruses that cause infections with similar symptoms, like ZIKV and dengue virus (DENV) (*1*). Existing nucleic acid detection methods are very sensitive and rapidly adaptable, but most require extensive sample manipulation and expensive machinery (*1*, *6*–*8*). In contrast, antigen-based rapid diagnostic tests require minimal equipment but have lower sensitivity and specificity, and assay development can take months (*9*–*11*). An ideal diagnostic would combine the sensitivity, specificity, and flexibility of nucleic acid diagnostics with the speed and ease of use of antigen-based tests. Such a diagnostic could be rapidly developed and deployed in the face of emerging viral outbreaks and would be suitable for disease surveillance or routine clinical use in any context.

The Cas13-based nucleic acid detection platform SHERLOCK (specific high-sensitivity enzymatic reporter unlocking) has the potential to address the key challenges associated with viral diagnostics. SHERLOCK combines isothermal amplification via recombinase polymerase amplification (RPA) (*12*) with highly specific Cas13-based detection (Fig. 1A) (*13*). Cas13, an RNA-guided ribonuclease, provides specificity through CRISPR RNA (crRNA)–target pairing and additional sensitivity due to signal amplification by Cas13's collateral cleavage activity (*14*, *15*).

For SHERLOCK to excel at viral detection in any context, it should be paired with methods enabling direct detection from patient samples with a visual readout. In this study, we tested the performance of SHERLOCK for ZIKV and DENV detection in patient samples and developed HUDSON (heating unextracted diagnostic samples to obliterate nucleases), a method to enable rapid, sensitive detection of ZIKV and DENV directly from bodily fluids with a colorimetric readout, demonstrated as part of SHERLOCKv2 (*16*). Additionally, we designed SHERLOCK assays to distinguish multiple viral species and strains and identify clinically relevant mutations.

Detection of ZIKV and DENV in patient samples provides a stringent test of the sensitivity of SHERLOCK and its tolerance of viral diversity. Our ZIKV SHERLOCK assay had single-copy [1 copy (cp)/μl] sensitivity when tested on seed stock cDNA (fig. S1). We evaluated its performance on 40 cDNAs derived from samples collected during the 2015–2016 ZIKV pandemic, 37 from samples obtained from patients with suspected ZIKV infections and 3 from mosquito pools (Fig. 1B, fig. S2, and table S1). For 16 samples from these patients, we benchmarked SHERLOCK by comparing its sensitivity and specificity to those of other nucleic acid amplification tests, including the commercially available Altona Realstar ZIKV reverse transcription polymerase chain reaction (RT-PCR) assay (Fig. 1C, figs. S3 to S5, table S2, and supplementary text). Of the 10 samples that tested positive by the Altona assay, all 10 were detected by SHERLOCK (100% sensitivity); the other 6 samples were negative by both assays (100% specificity, 100% concordance). Our ZIKV assay had no false positives when tested on healthy urine and water (Fig. 1B). We then validated the ability of SHERLOCK to detect DENV, a related but more diverse flavivirus that causes symptoms similar to those of ZIKV infection. All 24 RT-PCR–positive DENV RNA samples were confirmed to be positive for DENV after 1 hour of detection (Fig. 1D, figs. S6 and S7, and table S3). SHERLOCK sensitively and specifically detects viral nucleic acids extracted from ZIKV and DENV patient samples.

Although SHERLOCK excels at detecting extracted nucleic acids, a field-deployable, rapid diagnostic test should not require an extraction step to detect viral nucleic acid in bodily fluids. Many viruses, including ZIKV and DENV, are shed in urine or saliva, and sampling is not invasive (*2*, *7*). To detect viral nucleic acid directly from bodily fluids via SHERLOCK, we developed HUDSON, a method to lyse viral particles and inactivate the high levels of ribonucleases found in bodily fluids with the use of heat and chemical reduction (Fig. 2A and fig. S8) (*17*). HUDSON-treated urine or saliva could be directly added to RPA reaction mixtures with no dilution or purification step [blood products were diluted 1:3 in phosphate-buffered saline (PBS) to avoid solidification during HUDSON] without inhibiting subsequent amplification or detection. HUDSON and SHERLOCK enabled sensitive detection of free ZIKV nucleic acid spiked into

[1]Broad Institute of the Massachusetts Institute of Technology (MIT) and Harvard, Cambridge, MA 02142, USA. [2]Center for Systems Biology, Department of Organismal and Evolutionary Biology, Harvard University, Cambridge, MA 02138, USA. [3]Ph.D. Program in Virology, Division of Medical Sciences, Harvard Medical School, Boston, MA 02115, USA. [4]Department of Systems Biology, Harvard Medical School, Boston, MA 02115, USA. [5]McGovern Institute for Brain Research, MIT, Cambridge, MA 02139, USA. [6]Department of Brain and Cognitive Science, MIT, Cambridge, MA 02139, USA. [7]Department of Biological Engineering, MIT, Cambridge, MA 02139, USA. [8]Department of Health Sciences and Technology, MIT, Cambridge, MA 02139, USA. [9]Department of Electrical Engineering and Computer Science, MIT, Cambridge, MA 02139, USA. [10]Institute for Medical Engineering and Science, MIT, Cambridge, MA 02139, USA. [11]Department of Biological Sciences, Florida Gulf Coast University, Fort Myers, FL 33965, USA. [12]Centro de Investigaciones Genética, Instituto de Investigacion en Microbiologia, Universidad Nacional Autónoma de Honduras, Tegucigalpa, Honduras. [13]Department of Immunology and Infectious Disease, Harvard School of Public Health, Boston, MA 02115, USA. [14]Araraquara Laboratory of Public Health, School of Pharmaceutical Sciences, São Paulo State University, São Paulo, Brazil. [15]Laboratorio de Pesquisas em Virologia, Faculdade de Medicina de Sao Jose do Rio Preto, São Paulo, Brazil. [16]Department of Medicine, Mount Sinai School of Medicine, New York, NY 10029, USA. [17]Department of Microbiology and Immunobiology, Harvard Medical School, Boston, MA 02115, USA. [18]Howard Hughes Medical Institute (HHMI), Chevy Chase, MD 20815, USA.
*These authors contributed equally to this work.
†Corresponding author. Email: pardis@broadinstitute.org (P.C.S.); cmyhrvol@broadinstitute.org (C.M.); cfreije@broadinstitute.org (C.A.F.) ‡These authors contributed equally to this work.

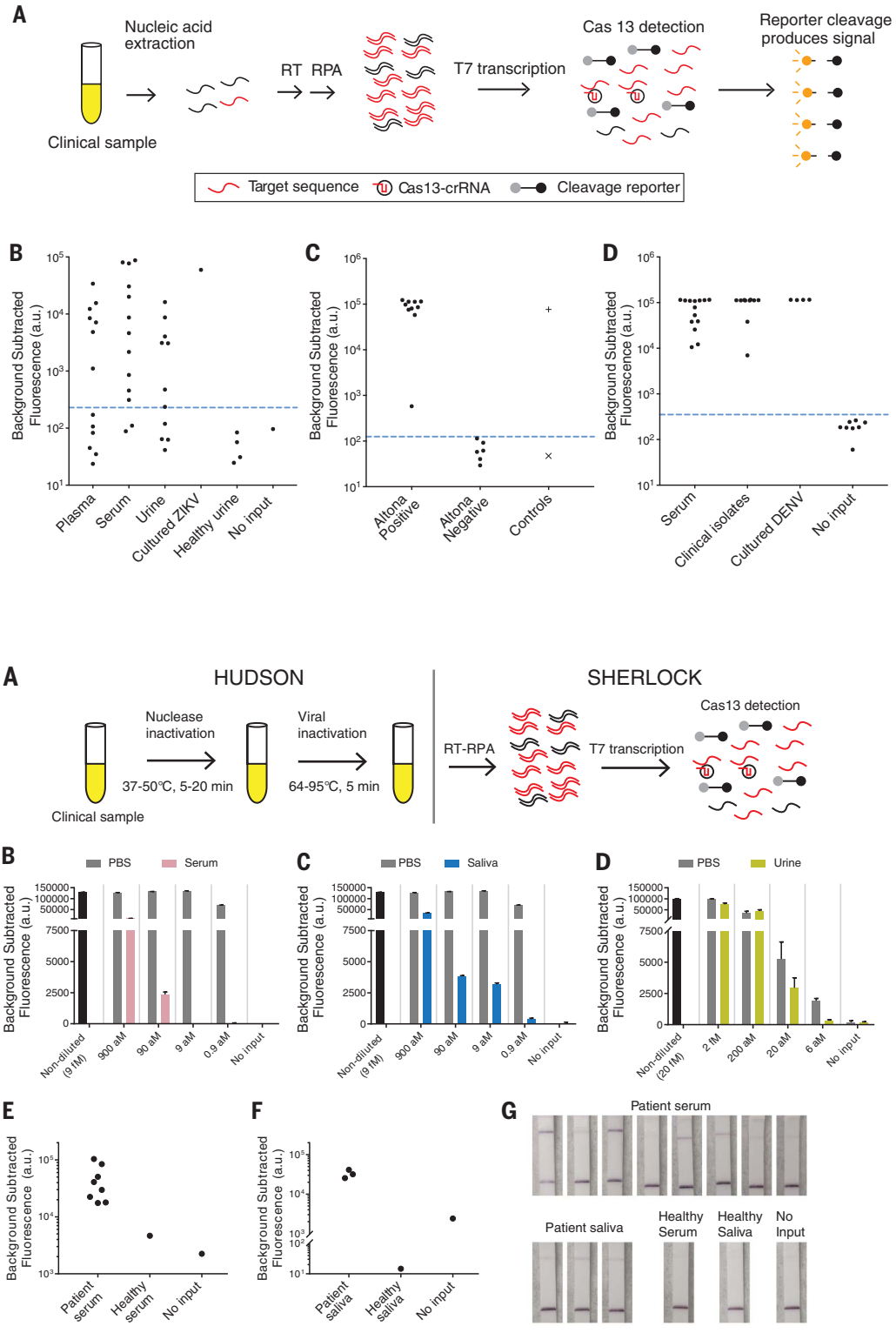

Fig. 1. ZIKV and DENV detection from patient samples and clinical isolates. (**A**) Schematic of SHERLOCK. Nucleic acid is extracted from clinical samples, and the target is amplified by RPA with either RNA or DNA as the input (RT-RPA or RPA, respectively). RPA products are detected in a reaction mixture containing T7 RNA polymerase, Cas13, a target-specific crRNA, and an RNA reporter that fluoresces when cleaved. We tested SHERLOCK on (**B**) cDNAs derived from 37 patient samples collected during the 2015–2016 ZIKV pandemic and (**C**) cDNAs from 16 patient samples for which results were compared head-to-head to those from the Altona RealStar ZIKV RT-PCR assay. +, ZIKV seed stock cDNA (3×10^2 cp/μl); ×, no input; a.u., arbitrary units. (**D**) SHERLOCK testing of RNA extracted from 24 DENV-positive patient samples and clinical isolates. Dashed blue line: threshold for detecting the presence or absence of ZIKV or DENV (see methods in the supplementary materials).

Fig. 2. Direct detection of ZIKV and DENV in bodily fluids with HUDSON and SHERLOCK. (**A**) Schematic of direct viral detection by HUDSON and SHERLOCK. (**B** and **C**) Detection of ZIKV RNA in particles diluted in healthy human serum (B) or healthy human saliva (C). The same PBS control was used for (B) and (C) as experiments were performed together. (**D**) Detection of ZIKV RNA in particles diluted in healthy human urine. Error bars indicate 1 SD for three technical replicates. (**E** and **F**) Detection of DENV RNA directly from patient serum (E) and saliva (F) samples. (**G**) Lateral-flow detection of DENV from the samples represented in (E) and (F). All samples were treated with tris(2-carboxyethyl)phosphine hydrochloride (TCEP)–EDTA before being heated.

urine, whole blood, plasma, serum, or saliva (figs. S9 and S12). To mimic clinical infection, where viral nucleic acid is encapsulated in infectious particles, we spiked infectious ZIKV particles into bodily fluids. HUDSON combined with SHERLOCK (figs. S13 and S14) permitted sensitive detection of ZIKV RNA from infectious particles at 90 aM (45 cp/μl) in whole blood (fig. S15) or serum (Fig. 2B), 0.9 aM (~1 cp/μl) in saliva (Fig. 2C), and 20 aM (10 cp/μl) in urine. The total turnaround time was <2 hours with fluorescent and colorimetric readouts (Fig. 2D and fig. S16). The sensitivity of HUDSON and SHERLOCK is comparable to ZIKV RNA concentrations observed in patient samples, which range from 1 to 1,000 cp/μl (*1*, *2*). HUDSON, paired with the pan-DENV SHERLOCK assay, detected DENV in whole blood, serum, and saliva (figs. S17 and S18). DENV was detected directly from eight of eight patient serum samples (Fig. 2E) and three of three patient saliva samples (Fig. 2F) tested, with

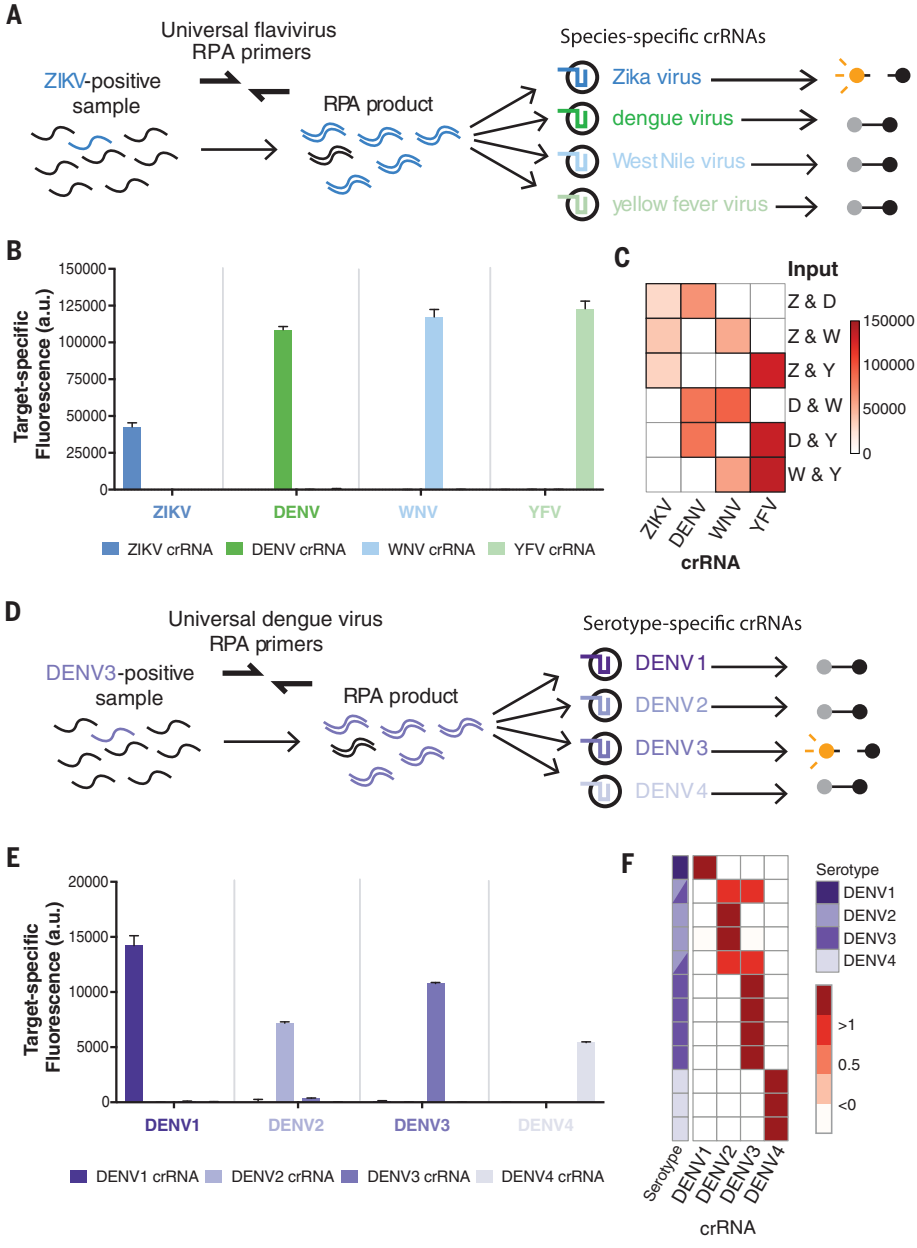

Fig. 3. Multivirus panels can be used to differentiate viral species and serotypes. (**A** to **C**) Panel of four related flaviviruses (A) used to detect individual viral targets (B) or paired viral targets (C) with species-specific crRNAs after 3 hours. Z, ZIKV; D, DENV; W, WNV; Y, YFV. (**D** and **E**) Identification of DENV serotypes 1 through 4 with the use of serotype-specific crRNAs (D), tested with the use of synthetic targets after 3 hours (E). (**F**) Identification of DENV serotypes in RNA extracted from patient samples. Each row represents a sample, each column represents a crRNA, and target-specific fluorescence values are normalized by row. Purple: DENV serotype identified. Synthetic targets were used at 10^4 cp/μl. Error bars indicate 1 SD for three technical replicates. We expect off-target crRNAs to have close to zero target-specific fluorescence (see methods in the supplementary materials). Primer, crRNA, and target sequences are in tables S5 to S7.

a total turnaround time of <1 hour for saliva despite lower viral titers than those in serum (*7*). We directly detected DENV with a colorimetric readout using lateral-flow strips (Fig. 2G), showcasing a HUDSON-to-SHERLOCK pipeline that can detect ZIKV or DENV directly from bodily fluids with minimal equipment.

Because many genetically and antigenically similar flaviviruses cocirculate and cause similar symptoms, we developed diagnostic panels to distinguish related viral species and serotypes. We identified conserved regions within ZIKV, DENV, West Nile virus (WNV), and yellow fever virus (YFV) genomes and designed a flavivirus panel with universal flavivirus RPA primers that can amplify any of the four viruses and species-specific crRNAs (Fig. 3A). This panel detected synthetic ZIKV, DENV, WNV, and YFV DNA targets with <0.22% off-target fluorescence (Fig. 3B, figs. S19 and S20, and methods in the supplementary materials) and identified the presence of all pairwise combinations of these four viruses, demonstrating the ability to detect mock coinfections (Fig. 3C and figs. S21 and S22). We also designed a DENV panel with DENV-specific RPA primers and serotype-specific crRNAs (Fig. 3D) that could distinguish between DENV serotypes 1 through 4 with <3.2% off-target fluorescence (Fig. 3E and figs. S23 and S24). This low level of off-target fluorescence allows for 100% specificity in differentiating among serotypes, providing an alternative to current serotype identification approaches (*8*). The DENV panel confirmed the serotypes of 12 RT-PCR–serotyped patient samples or clinical isolates (Fig. 3F and fig. S25) and identified two clinical isolates with mixed infection, a commonly observed phenomenon (*18*). SHERLOCK can therefore be extended to differentiate between related viruses or serotypes with a single amplification reaction.

SHERLOCK is poised for field-deployable variant identification, which would allow real-time tracking of microbial threats. Genotyping of single-nucleotide polymorphisms (SNPs) typically involves PCR and either fluorescence- or mass spectrometry–based detection, requiring extensive sample processing and expensive equipment and limiting field deployability (*19*). SHERLOCK can identify SNPs by placing a synthetic mismatch in the crRNA near the SNP and testing each target with ancestral target-specific and derived target-specific crRNAs (Fig. 4A) (*13*). We designed diagnostics for three region-specific SNPs from the 2015–2016 ZIKV pandemic (Fig. 4B) and identified these SNPs in synthetic targets, a viral seed stock, and cDNA samples from Honduras, the Dominican Republic, and the United States (Fig. 4, C to E). These results

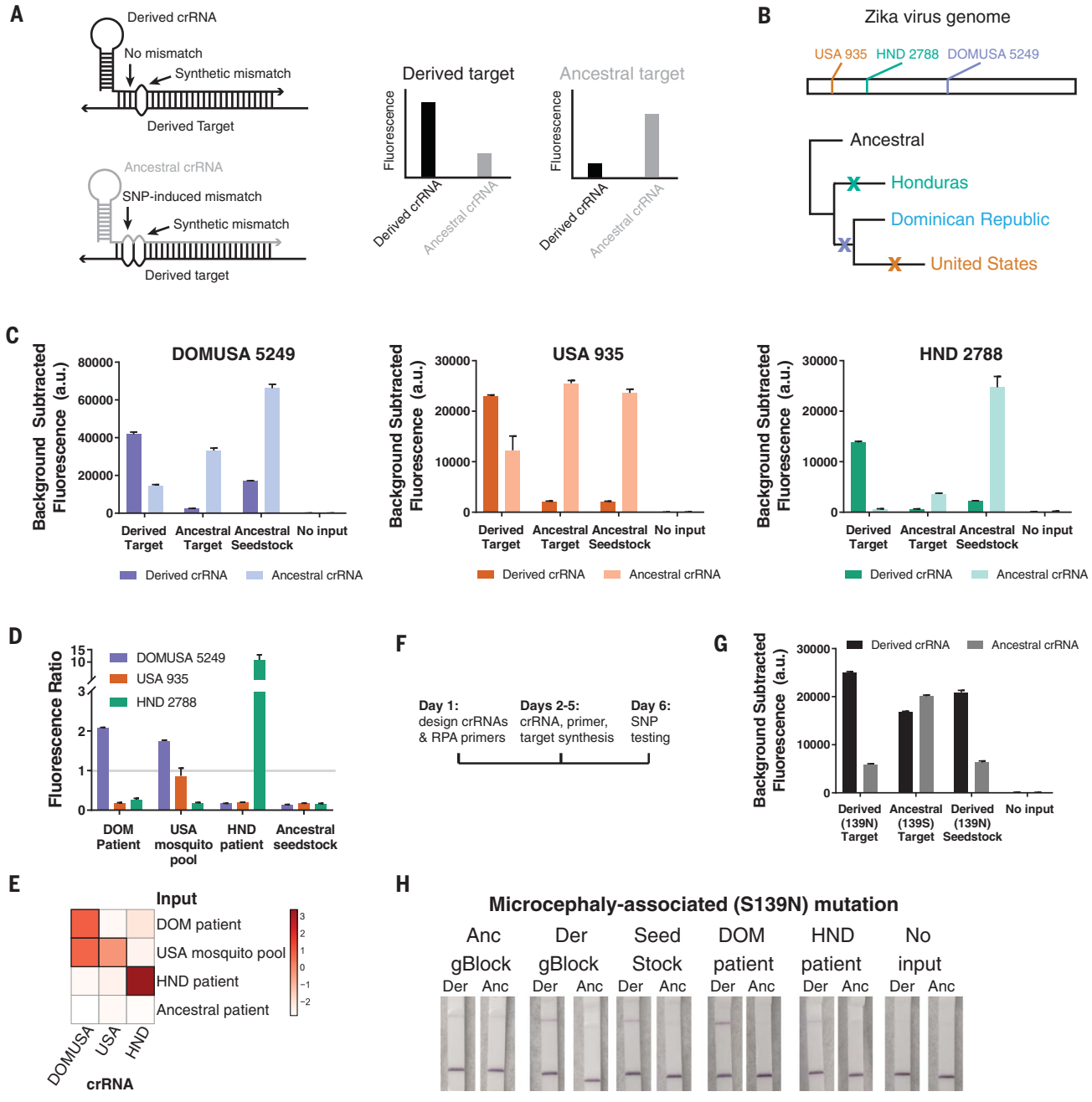

Fig. 4. Identification of adaptive and functional ZIKV mutations. (**A**) SHERLOCK assays for SNP identification. (**B** and **C**) Three region-specific SNPs from the 2015–2016 ZIKV pandemic, including genomic locations of the SNPs and a simplified phylogenetic tree, tested with the use of synthetic targets (10^4 cp/μl) and viral seed stock cDNA (3×10^2 cp/μl). (**D** and **E**) Identification of region-specific SNPs in ZIKV cDNA samples from the Dominican Republic (DOM), the United States, and Honduras (HND). The fluorescence ratio (derived crRNA fluorescence divided by ancestral crRNA fluorescence) for each SNP in each sample is shown in a bar plot (log_2-transformed data in a heatmap). (**F**) Timeline for developing a SHERLOCK assay for a new SNP (more detail in fig. S26). (**G** and **H**) Identification of a microcephaly-associated ZIKV mutation (PrM S139N) by fluorescence and colorimetric detection. In all panels, error bars indicate 1 SD for three technical replicates. Anc, ancestral; Der, derived; gBlock, gene fragment.

demonstrate that SHERLOCK can identify SNPs in samples from the ZIKV pandemic and highlight the single-nucleotide specificity of SHERLOCK.

Rapid identification of emerging drug resistance and other clinically relevant mutations for viruses such as ZIKV and HIV would have great utility. A ZIKV point mutation in the PrM protein region [Ser^{139}→Asn (S139N)] recently reported to be associated with fetal microcephaly (*20*) was used as a test case for the rapid development of assays for variant identification. Within a week of the report's publication (Fig. 4F and fig. S26), we developed multiple SHERLOCK assays for the S139N mutation (Fig. 4G and fig. S27) and could identify the mutation in patient samples from the 2015–2016 ZIKV pandemic with a visual readout (Fig. 4H). To further illustrate the ease of developing SHERLOCK diagnostics for many clinically relevant mutations, we designed and tested assays for the six most commonly observed drug resistance mutations in HIV reverse transcriptase

(*21*) in 1 week (fig. S28). These examples underscore the potential for SHERLOCK to be used for monitoring clinically relevant variants in near real time.

Combining HUDSON and SHERLOCK, we have created a field-deployable viral diagnostic platform with high performance and minimal equipment or sample processing requirements. This platform is as sensitive and specific as amplification-based nucleic acid diagnostics (*12*, *22*–*26*), with speed and equipment requirements similar to those of rapid antigen tests (*9*–*11*). Furthermore, this approach can be easily adapted to detect virtually any virus present in bodily fluids and scaled to enable multiplexed detection (*16*), and the reagents can be lyophilized for cold-chain independence (*13*). Cas13-based detection is a promising next-generation diagnostic strategy with the potential to be implemented almost anywhere in the world to enable effective, rapid diagnosis of viral infections.

REFERENCES AND NOTES

1. O. Faye *et al*., *J. Clin. Virol.* **43**, 96–101 (2008).
2. G. Paz-Bailey *et al*., *N. Engl. J. Med.* NEJMoa1613108 (2017).
3. H. C. Metsky *et al*., *Nature* **546**, 411–415 (2017).
4. N. R. Faria *et al*., *Nature* **546**, 406–410 (2017).
5. N. D. Grubaugh *et al*., *Nature* **546**, 401–405 (2017).
6. O. Faye *et al*., *Virol. J.* **10**, 311 (2013).
7. A.-C. Andries *et al*., *PLOS Negl. Trop. Dis.* **9**, e0004100 (2015).
8. J. J. Waggoner *et al*., *J. Clin. Microbiol.* **51**, 3418–3420 (2013).
9. I. Bosch *et al*., *Sci. Transl. Med.* **9**, eaan1589 (2017).
10. A. Balmaseda *et al*., *Proc. Natl. Acad. Sci. U.S.A.* **114**, 8384–8389 (2017).
11. L. Priyamvada *et al*., *Proc. Natl. Acad. Sci. U.S.A.* **113**, 7852–7857 (2016).
12. O. Piepenburg, C. H. Williams, D. L. Stemple, N. A. Armes, *PLOS Biol.* **4**, e204 (2006).
13. J. S. Gootenberg *et al*., *Science* **356**, 438–442 (2017).
14. O. O. Abudayyeh *et al*., *Science* **353**, aaf5573 (2016).
15. A. East-Seletsky *et al*., *Nature* **538**, 270–273 (2016).
16. J. S. Gootenberg *et al*., *Science* **360**, 439–444 (2018).
17. J. L. Weickmann, D. G. Glitz, *J. Biol. Chem.* **257**, 8705–8710 (1982).
18. R. Requena-Castro, M. Á. Reyes-López, R. E. Rodríguez-Reyna, P. Palma-Nicolás, V. Bocanegra-García, *Mem. Inst. Oswaldo Cruz* **112**, 520–522 (2017).
19. S. Kim, A. Misra, *Annu. Rev. Biomed. Eng.* **9**, 289–320 (2007).
20. L. Yuan *et al*., *Science* **358**, 933–936 (2017).
21. S.-Y. Rhee *et al*., *Nucleic Acids Res.* **31**, 298–303 (2003).
22. Y. Du *et al*., *Angew. Chem. Int. Ed.* **56**, 992–996 (2017).
23. K. E. Eboigbodin, M. Brummer, T. Ojalehto, M. Hoser, *Diagn. Microbiol. Infect. Dis.* **86**, 369–371 (2016).
24. K. Pardee *et al*., *Cell* **165**, 1255–1266 (2016).
25. N. Chotiwan *et al*., *Sci. Transl. Med.* **9**, eaag0538 (2017).
26. J. Van Ness, L. K. Van Ness, D. J. Galas, *Proc. Natl. Acad. Sci. U.S.A.* **100**, 4504–4509 (2003).

ACKNOWLEDGMENTS

We thank S. Schaffner, A. Lin, and other Sabeti lab members for useful feedback; J. Strecker for providing SUMO protease; and the Florida Department of Health, Miami-Dade County Mosquito Control, and Boca Biolistics for support with patient and mosquito samples. **Funding:** We acknowledge funding from HHMI, the Broad Institute Chemical Biology and Therapeutics Science Shark Tank, NIH grant U19AI110818, and Defense Advanced Research Projects Agency grant D18AC00006. The views, opinions, and/or findings expressed should not be interpreted as representing the official views or policies of the Department of Defense or the U.S. government. This study has been approved for public release; distribution is unlimited. C.M. is supported by HHMI. O.O.A. is supported by a Paul and Daisy Soros fellowship and NIH grant F30 NRSA 1F30-CA210382. S.I. and S.F.M. are supported by NIH National Institute of Allergy and Infectious Diseases grant R01AI099210. I.B. and L.G. are supported by NIH grant AI 100190. F.Z. is supported by NIH grants 1R01-HG009761, 1R01-MH110049, and 1DP1-HL141201; HHMI; the New York Stem Cell, Allen, and Vallee foundations; the Tan-Yang Center at MIT; and J. and P. Poitras and R. Metcalfe. F.Z. is a New York Stem Cell Foundation–Robertson Investigator. M.L.N. is supported by the Sao Paulo Research Foundation (FAPESP; grant 13/21719-3) and is a Conselho Nacional de Desenvolvimento Científico e Tecnológico (CNPq) Research Fellow. **Author contributions:** C.M. and C.A.F. conceived the study, performed experiments and data analysis (supervised by P.C.S.), and wrote the paper (with P.C.S and B.L.M.). J.S.G. and O.O.A. designed some experimental protocols, provided reagents, and gave technical advice (supervised by F.Z.). H.C.M. assisted with crRNA and RPA primer design and analysis of ZIKV genome coverage. M.J.K. purified Cas13 proteins used in this study. A.F.D. cultured and titered the ZIKV used in this study (supervised by I.B. and L.G.). A.L.T., L.M.P., K.G.B., B.C., B.L.M., N.L.Y., A.M., M.L.N., S.I., S.F.M., L.A.P., K.F.G., L.G., I.B., and I.L. provided critical insights or clinical samples used in this study. All authors reviewed the manuscript. **Competing interests:** C.M., C.A.F., P.C.S., J.S.G., O.O.A., and F.Z. are co-inventors on patent applications filed by the Broad Institute relating to work in this study. **Data and materials availability:** All data are available in the article or the supplementary materials. Details on material transfer agreements related to the sharing of clinical samples are provided in the methods section in the supplementary materials.

SUPPLEMENTARY MATERIALS

www.sciencemag.org/content/360/6387/444/suppl/DC1
Materials and Methods
Supplementary Text
Figs. S1 to S28
Tables S1 to S7
References (*27*–*31*)

2 January 2018; resubmitted 20 February 2018
Accepted 8 March 2018
10.1126/science.aas8836

Science

Field-deployable viral diagnostics using CRISPR-Cas13

Cameron Myhrvold, Catherine A. Freije, Jonathan S. Gootenberg, Omar O. Abudayyeh, Hayden C. Metsky, Ann F. Durbin, Max J. Kellner, Amanda L. Tan, Lauren M. Paul, Leda A. Parham, Kimberly F. Garcia, Kayla G. Barnes, Bridget Chak, Adriano Mondini, Mauricio L. Nogueira, Sharon Isern, Scott F. Michael, Ivette Lorenzana, Nathan L. Yozwiak, Bronwyn L. MacInnis, Irene Bosch, Lee Gehrke, Feng Zhang and Pardis C. Sabeti

Science **360** (6387), 444-448.
DOI: 10.1126/science.aas8836

Taking CRISPR technology further

CRISPR techniques are allowing the development of technologies for nucleic acid detection (see the Perspective by Chertow). Taking advantages of the distinctive enzymatic properties of CRISPR enzymes, Gootenberg *et al.* developed an improved nucleic acid detection technology for multiplexed quantitative and highly sensitive detection, combined with lateral flow for visual readout. Myhrvold *et al.* added a sample preparation protocol to create a field-deployable viral diagnostic platform for rapid detection of specific strains of pathogens in clinical samples. Cas12a (also known as Cpf1), a type V CRISPR protein, cleaves double-stranded DNA and has been adapted for genome editing. Chen *et al.* discovered that Cas12a also processes single-stranded DNA threading activity. A technology platform based on this activity detected human papillomavirus in patient samples with high sensitivity.

Science, this issue p. 439, p. 444, p. 436; see also p. 381